Assessment of the Illumination and Communication Performance of a Visible Light System in an Indoor Scenario

David Esteban Farfan-Guillen[1] , Paulo de Tarso Neves Junior[1] , Alexandre de Almeida Prado Pohl[1]

[1]*Graduate Program in Electrical and Computer Engineering (CPGEI), Universidade Tecnológica Federal do Paraná (UTFPR), Curitiba, Brazil.*
davides.far@gmail.com, pneves@utfpr.edu.br, pohl@utfpr.edu.br

Abstract— **Visible-light communication (VLC) is a technique that employs light-emitting diodes (LEDs) and photodiodes to enable communication in indoor scenarios. VLC has gathered increasing attention due to its potential for data transmission across a broad unregulated spectrum (430-790 THz). One of VLC's primary objectives is to utilize pre-existing LED infrastructures as access points. In this investigation, we assess the performance of an indoor VLC link by measuring the illumination characteristics of commercial LED luminaire. The results are utilized to design an electronic transmission and reception circuit. An analysis was conducted to identify the optimal operating point that ensures adequate lighting and reliable communication. The designed circuits exhibited a bandwidth of 50 MHz at -3 dB. Characterization of the luminaire demonstrated that a single luminaire provided the illumination (486 lx) within the recommended range at 1.6 m. For data transmission, the variable pulse position modulation (VPPM) and the orthogonal frequency-division multiplexing (OFDM) were employed in different configurations. The bit error rate (BER) results, with a threshold of $\leq 10^{-3}$, revealed that VPPM performed best at a distance of 1.9 m with a rate of 12.5 Mbps. Conversely, OFDM modulation achieved optimal performance at 1.75 m, providing a transmission rate of 30 Mbps.**

Index Terms—Illumination, Indoor Communication, Light-Emitting Diodes, Visible light Communication.

I. INTRODUCTION

Wireless communications have witnessed remarkable progress in recent years, partly due to the widespread use of the internet and the availability of numerous network-connected devices. Wireless connectivity has successfully enabled various telecommunication technologies, supporting a wide range of services that demand higher transmission bandwidth [1]. It can be categorized into two types: radio frequency (RF) and optical wireless communication (OWC) [2]. RF communication has been extensively developed; however, as device connectivity grows, the frequency spectrum becomes more congested, restricting its current capacity. Consequently, alternative or complementary technologies to RF have been explored to overcome the impending congestion [3].

In the realm of OWC, visible light communication (VLC) utilizes light-emitting diodes (LEDs) in the visible spectrum to transmit data [4]. With its large bandwidth (430-790 THz), it offers the potential to complement RF technologies, providing various solutions [5] that can work efficiently

alongside other wireless technologies, such as Wi-Fi, Long-Term Evolution (LTE), 5G and 6G [6]. It has been standardized under IEEE 802.15.7, ensuring compatibility with both existing and future networks. Among the advantages, VLC employs the existing infrastructure, as LED devices serve the dual purpose of lighting and communication [3], which contribute to energy savings compared to older lighting technologies, making it an environmental friendly option [7]. Additionally, VLC provides enhanced security as the signal does not penetrate opaque objects such as walls, making it suitable for secure indoor applications in healthcare facilities, airplanes, underwater communications and oil refineries [8]. It operates in an unregulated spectrum and does not cause electromagnetic interference.

Extensive research on VLC have addressed different aspects of the technique. Studies conducted by Haigh [9] and Azhar [10] have assessed the data transmission capabilities. Other studies, such as those by Bian [11] and Wei [12], have reported data rates in the gigabit per second range using different techniques, although the achieved distances are relatively short. To improve the channel performance, researchers have explored the use of lenses to extend the communication range [13]. Other studies have investigated the technique in underwater [14], underground mining [15] and vehicular communication [16], [17], as well as in positioning [18], transmission of 5G signals [19], and in the Internet of Things (IoT) paving the way to consolidate the Light-Fidelity (Li-Fi) network [20].

In indoor applications, luminaires that contain several discrete LEDs can serve as wireless access points for implementing VLC systems [4]. However, there are still few studies that utilize commercial LED luminaires in experiments. For instance, an analysis of a VLC link with a commercial luminaire employing OOK modulation was presented in [21]. Another study focused on the simulation of the light emission of a commercial luminaire using the APEX software [22], but without considering the transmission rate. However, the lack of information concerning both illumination and transmission aspects hinders the practical application of VLC in real-world scenarios. To ensure its successful implementation, research efforts must focus on characterizing the transmitting (LED luminaires) and receiving elements (photodiodes) that impact the channel performance, as well as as on the analysis of the illumination condition during data communication. Given these constraints, it is crucial for the telecom and lighting industries to collaborate and standardize devices that facilitate the commercial development of the technique [23].

The objective of this study is to design VLC links for indoor spaces that fulfills the dual functionality of providing adequate lighting conditions while enabling high-speed data transmission. A commercial LED luminaire, specifically the SP-02-T1 SinkPAD-II LED model [24], equipped with seven high-power white LEDs (LX18-P150-3) and a polycarbonate concentrator [22], was used for this purpose. The luminaire was extensively characterized concerning the spread of light, and based on its performance, electronic circuits were designed to achieve a high data rate while maintaining optimal lighting conditions.

The analysis of the VLC link was performed using the LED luminaire mentioned above and a photodiode (Thorlabs, model FDS 100 with a sensitivity of 0.65 A/W - 20 V and with an active area of 13 mm^2) [25]. An experimental photometric analysis was performed to evaluate the emitted spectrum and the optical power of the LED luminaire, as well as the power received by the photodiode at the receiving end. Other parameters, such as the signal-to-noise ratio (SNR), bit error rate (BER), and data rate, were also assessed. By considering such an information, both the communication performance and lighting characteristics were evaluated. The results demonstrate that the LED luminaire achieves

the required level of performance and functionality for employment in indoor scenarios.

This work is organized as follows. After the introduction in Section 1, Section 2 describes the optical wireless channel. Section 3 describes the characterization of the LED luminaire and the photodiode, followed by Section 4 that presents the design of the electronic circuits used in the transmission and reception tests. Section 5 shows the results and analysis of the VLC link performance and Section 6 brings the discussion and conclusions of this study.

II. THE OPTICAL WIRELESS CHANNEL

The VLC channel consists of a LED transmitter that modulates the data, and a receiver, in which a photodetector is responsible for capturing the transmitted light and converting it into electrical energy. We assume that the channel is linear, time-invariant, and without memory [26] and a line-of-sight (LoS) scenario. As the wavelength used for transmission is smaller than the photodetector area, the system experiences slow fading [7]. The channel can be mathematically represented by the continuous-time equation:

$$y(t) = h(t) * R \cdot x(t) + n(t), \tag{1}$$

where $y(t)$ represents the received signal after passing through the optical wireless channel plus noise. $x(t)$ represents the transmitted signal, R is the photodetector responsivity, $h(t)$ represents the impulse response of the channel, and $n(t)$ represents to the additive white Gaussian noise (AWGN) that affects the signal.

Fig. 1 illustrates the indoor scenario of the LoS VLC channel, where d represents the distance between the transmitter and the receiver, r is the radius of the photodetector area, α denotes the incidence angle, and ϕ represents the radiated viewing angle. According to [26], in a scenario where the transmitter
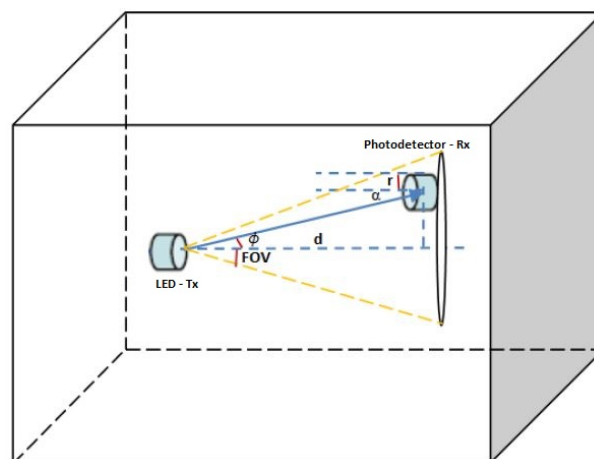

Fig. 1. VLC system - LoS scenario for an indoor application

exhibits a Lambertian emission pattern and the receiver is located at distance d, the signal attenuation over the optical path can be described by equation (2)

$$H_{LoS}(0) = \frac{(m+1) \cdot A_r}{2\pi \cdot d^2} \cdot \cos^m \phi \cdot \cos \alpha, \tag{2}$$

in which Ar is the effective area of the photodetector, ϕ is the irradiation angle, and α is the incidence angle [27]. In equation (2), also known as the channel gain, m represents the Lambertian emission

order, which relies on the source's half-power angle ($\phi_{(1/2)}$), expressed as

$$m = -\frac{ln(2)}{ln(\cos(\phi_{1/2}))}. \tag{3}$$

Equation (3) determines the order parameter m as a function of the half-power ($\phi_{(1/2)}$) and is used to characterize the angular dispersion of the transmitted light. To assess the VLC link performance, the received power (P_r) is obtained by multiplying the channel gain, H_{LoS} by the input optical power, P_t, as described in equation (4).

$$P_r = H_{LoS}(0) \cdot P_t. \tag{4}$$

In indoor VLC links the noise is modeled as additive white Gaussian noise (AWGN), originating from ballistic noise, including the ambient light contribution, and the thermal noise from the receiver amplifier [28].

$$\sigma^2_{total} = \sigma^2_{thermal} + \sigma^2_{ballistic}. \tag{5}$$

Thus, the signal-to-noise ratio (SNR) is expressed by equation (6), where a higher SNR indicates better performance in the communication channel [29]. This relationship is used to quantify the ratio of the squared product of the received optical power, Pr, and the photodiode responsivity, R, over the total noise power, σ^2_{total}.

$$SNR = \frac{(P_r \cdot R)^2}{\sigma^2_{total}}. \tag{6}$$

In terms of data transmission, both single-carrier and multicarrier modulation techniques can be employed [26] [30]. For single-carrier modulation, techniques that shape the pulse within the bit slot can be employed, such as the variable pulse position modulation (VPPM), which is a combination of pulse position modulation (PPM) and pulse width modulation (PWM) [31] [32]. In PPM, the bit interval is divided into subintervals of equal duration, and a pulse is transmitted within a specific subinterval to indicate the transmitted bit. PWM adjusts the pulse width based on the desired dimming level. For multicarrier modulation, the technique of orthogonal frequency division multiplexing (OFDM) can be utilized [33]. In this case, the channel is divided into multiple subcarriers with orthogonal frequencies. The data is modulated using an M-ary scheme, employing quadrature amplitude modulation (M-QAM) [34]. The IFFT transforms the input signal, initially in the frequency domain, into an output signal in the time domain. To mitigate intersymbol interference (ISI), a cyclic prefix (CP) is added. Signal recovery involves the reverse process, where the CP is removed, a Fast Fourier Transform (FFT) is applied, and the signal is demodulated.

The corresponding bit error rate (BER), derived for the VPPM and OFDM modulations, are expressed by (7) and (8), respectively.

$$\left\{ \begin{array}{ll} Q(\sqrt{\frac{SNR}{2 \cdot \alpha}}) & \alpha \leq 0,5 \\ Q(\sqrt{\frac{SNR \cdot (1-\alpha)}{2 \cdot \alpha^2}}) & \alpha > 0,5 \end{array} \right\}, \tag{7}$$

$$BER_{OFDM} = \frac{4}{\log_2 M} \cdot (1 - \frac{1}{\sqrt{M}}) \cdot Q(\sqrt{\frac{3\log_2 M}{M-1}SNR}), \tag{8}$$

where α represents the signal's duty cycle and Q is the Q-function [35], [36].

III. CHARACTERIZATION OF THE LED LUMINAIRE AND PHOTODIODE

This section reports on the characterization of the LED luminaire and the photodiode, with a focus on analyzing the lighting aspect, which is one of the attributes of VLC. The experiments seek to ensure that the lighting levels comply with the standards established for interior office environments, which range between 300 lx and 700 lx (typ 500 lx), according to the European standard [37]. We designed the transmission and reception circuits for data communication based on values obtained from these experiments. The analyzed parameters were the current range in which the LED emits light within the standard limits, as well as the corresponding optical power that the photodiode can receive.

In this study, we selected a commercial LED luminaire consisting of seven LEDs (model SP-02-T1SinkPad-II). We chose this luminaire because it emits white light, as recommended for indoor illumination. At the receiving side, we opted for a PIN photodiode (Thorlabs, model FDS100) due to its linear and stable response to incident light, as well as the easiness of applying the electrical polarization. This choice is important to ensure reliable detection of the optical signal in the VLC communication system. The SP-02-T1SinkPad-II LED luminaire features a round 40 mm downpad-II™ base and comprises seven LD LX18-P150 white light emitting elements. Its attributes include a 5000 K correlated color temperature (CCT), a 742 lm typical luminous flux, a 19.6 V typical feed voltage, a 350 mA typical polarization current, and a beam angle of 120°. As for the photodetector, the FDS100 is a high-speed silicon photodiode with a spectral response between 350 nm to 1100 nm. It has an active area of 13 mm² and shows rise times of approximately 10 ns with a 20V bias. The sensitivity response depends on the light wavelength, with a maximum response of 0.65 A/W at 950 nm.

A. Scenario

Experiments are performed envisaging an indoor application. We conducted tests on an optical table measuring 2x1 meters, and the working surface included a space of 3x2 meters around the table. Since the experiments took place inside a laboratory, the maximum distance covered was 2.2 m, and the maximum power supply to the luminaire was limited to 6 W.

B. Characterization of the LED luminaire

In the first experiment, we focused on testing the lighting performance by varying the direct current applied to the LED luminaire. These measurements aimed to determine the power density distribution, the optical power radiated over the area, and the illumination level. To measure the luminaire power spectrum we used the spectrometer, model CCS200 (Thorlabs). The LEDs work under the principle of phosphor-conversion, where the light emitted by a blue LED excites a yellow phosphor coating, resulting in a white light pattern. The power spectrum analysis revealed a peak at 580 nm, which corresponds to yellow light, and a peak at 454 nm, corresponding to the blue color, as shown in Fig. 2. We used the 580 nm peak as a reference for power measurements and circuit calculations.

For radiometric measurements, we employed a sensor head (model S121C, Thorlabs) with a responsivity of 3.79 mA/W at 580 nm. The maximum distance between the luminaire and the sensor head during the analysis was 2.2 m, as shown in Fig. 3 (a). To avoid interference of the laboratory lamps, whose power was previously measured to an average of 46 µW, we turned off the lamps and conducted the measurements without their influence. This was done to eliminate any background noise and to

Brazilian Microwave and Optoelectronics Society-SBMO   received 27 Jan. 2023; for review 09 Feb. 2023; accepted 06 Jul. 2023

Brazilian Society of Electromagnetism-SBMag   © 2023 SBMO/SBMag   (cc) BY   ISSN 2179-1074

ensure a reliable and accurate measurement without an impact on the transmitted signal. Also, there was no incidence of solar radiation in this scenario.
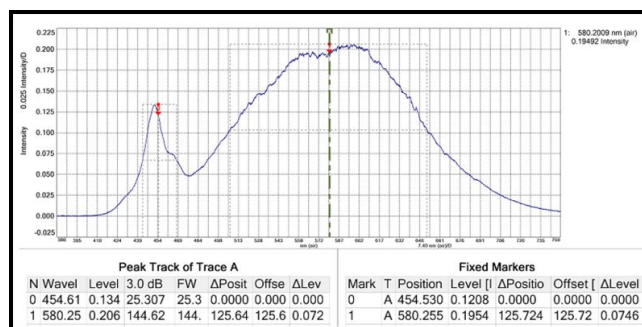

Fig. 2. Power spectrum distribution: the peak at 454 nm shows the emission of the blue LED. The peak at 580 nm corresponds to the emission of the yellow color.
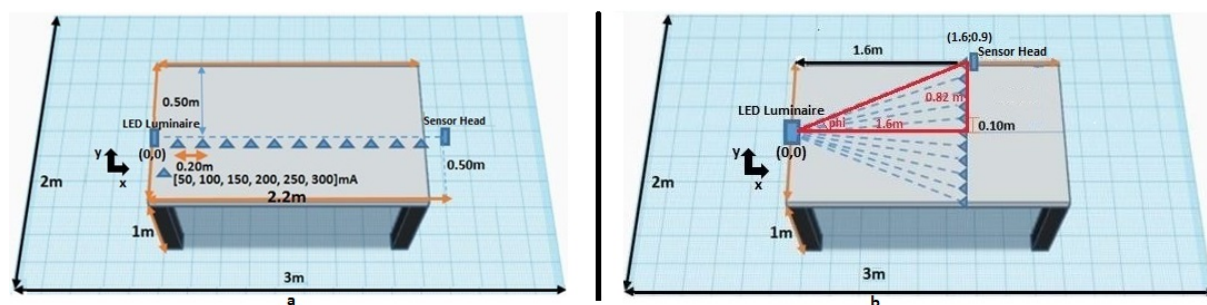

Fig. 3. (a) Scenario for the characterization of the luminaire optical power (b) Setup used to measure the angle of half power.

Fig. 4 (a) displays the results of the radiometric measurement of the optical power captured by the sensor head in the scenario depicted in Fig. 3 (a). The initial distance between the LED luminaire and the sensor was 0.20 m, and measurements were taken at intervals of 0.20 m up to a maximum distance of 2.2 m. The electric current supplied to the luminaire varied from 50 to 300 mA in increments of 50 mA. Table I shows the electrical power it consumed (the product of electric current and voltage), ranging from 1 to 6 W.

TABLE I. Experimental electric power applied in the LED luminaire.

Current (mA)	Voltage (V)		Electric Power (W)
50	18.7	=	0.93 (~1)
100	19.2	=	1.92 (~2)
150	19.6	=	2.94 (~3)
200	19.9	=	3.98 (~4)
250	20.2	=	5.05 (~5)
300	20.5	=	6.12 (~6)

Fig. 4 (a) illustrates the distribution of optical power in different ranges (represented by color-coded bars) based on the distance from the luminaire. We note that higher electrical power consumption (horizontal axis) results in higher received optical power. As the distance (vertical axis) between the luminaire and the sensor head increases, the optical power begins to decrease.
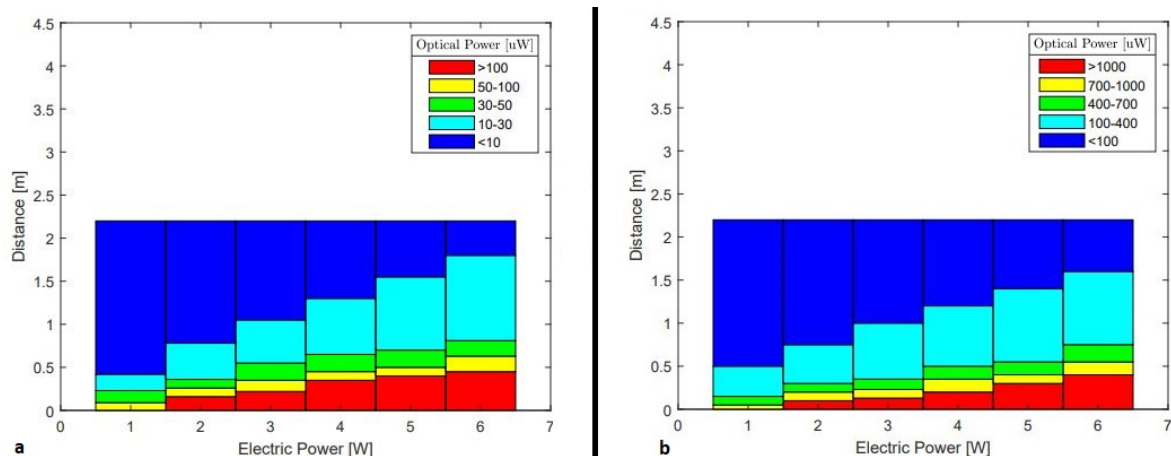
Fig. 4. (a) Variation of optical power with distance to the LED luminaire and electrical power (b) Optical power received by the photodiode at different electrical powers applied to the luminaire

Photometric measurements were conducted using a Criffer Flex X-08 lux meter to assess the illuminance characteristics in the scenario presented in Fig. 3 (a). In indoor areas, it is recommended to maintain lighting conditions between 300 and 700 lx (typ 500 lx), as per the European standard [37]. For the analysis, illuminance values equal to or greater than 500 lx were deemed suitable, as they match the level of typical illuminance. Table II displays the illuminance measured at distances up to 2.2 m. The highest performance was achieved at 1.6 m with an electrical power of P = 6 W (∼486 lx).

TABLE II. Illuminance given in lux units detected by the lux meter as a function of the distance to LED luminaire and variation of electrical power. The symbol > in the slots means measured values greater than 500 lux.

Electric Power	Distance (m)									
	0.4	0.6	0.8	1.0	1.2	1.4	1.6	1.8	2.0	2.2
1 W	>	348	160	141	113	89	74	64	56	48
2 W	>	>	425	376	301	236	198	171	149	128
4 W	>	>	>	>	499	370	324	266	224	205
6 W	>	>	>	>	>	>	486	359	280	264

With a single luminaire, it is observed that adequate lighting can be achieved up to a distance of 1.6 m, using an electrical power of P = 6 W. For lower powers, the distance required to meet the 500 lux requirement is shorter. However, by increasing the number of luminaires in a room, indoor lighting conditions can be satisfied.

To evaluate the medium power angle and Lambertian order of the luminaire, an experiment was conducted in which the sensor head was laterally moved while keeping the LED luminaire fixed. The distance between the luminaire and the sensor head was fixed at 1.6 m. The sensor head was moved laterally in steps of 0.10 m from the central axis, as depicted in Fig. 3 (b). The average power over the distance from the central axis was measured, and Fig. 5 shows the results. The power drop to half maximum occurs at approximately 0.82 m. By applying trigonometric relationships based on the grid lines shown in Fig. 5, the average power semi-angle was determined as 27.13°. The Lambertian order was estimated using equation (3), yielding a value of m = 5.94.
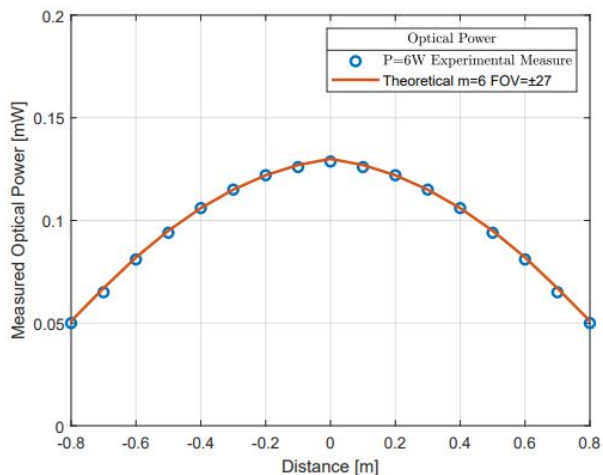
Fig. 5. Optical power measured with sensor head used to calculate the Lambertian m-order.

C. Photodiode Characterization

The FDS 100 photodiode (PD) was characterized in the scenario depicted in Fig. 3 (a). The circuit shown in Fig. 6 was built to measure the PD voltage in relation to the electrical power variation, controlled by the electric current of the DC source.
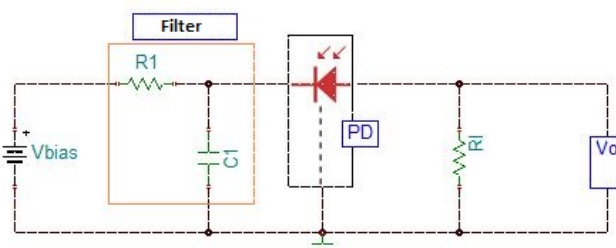

Fig. 6. Photodiode circuit used to measure changes in the optical response at the receiving side.

In the circuit, Vbias represents the reverse voltage supplied to the photodiode, and resistor R1 and capacitor C1 function as a high-pass filter. PD denotes the FDS 100 photodiode, and resistor Rl is the load resistance used to measure the voltage difference.

The current was calculated at different distances using the known values of voltage and resistance, following Ohm's law. The results are shown in Fig. 7. In the experiment, the LED luminaire remained fixed, and the PD circuit was moved in a straight line at intervals of 0.20 m up to 2.2 m. For instance, based on the data presented in Fig. 7, at an electric power of 6 W and a distance of 2.2 m, the photodiode circuit measured 2.04 μA. This corresponds to the minimum value at which the circuit can recover a signal in the employed setup. Furthermore, the amount of optical power received by the photodiode was calculated based on the photocurrent measurements, as shown in Fig. 4 (b), considering an effective area of 13 mm^2. It is evident that the received optical power (represented by different colored bars) is directly proportional to the electrical power consumed by the luminaire and inversely proportional to the distance between the luminaire and the photodiode.

The results presented in this section demonstrate that the LED luminaire exhibits Lambertian behavior, which is the characteristic of LED sources used in VLC implementations. Based on the experimental results, it was determined that the transmission circuit should be designed to operate within the range
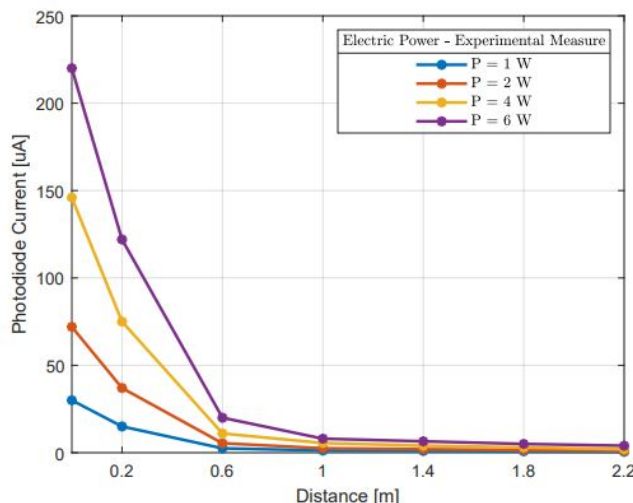
Fig. 7. Photocurrent calculated at the photodiode as a function of the distance to the LED luminaire considering the variation of the electrical power.

of 0 - 300 mA, ensuring compliance with the lighting standards. As for the reception circuit, it needs to be properly designed to amplify a signal with a photocurrent of up to 2.04 μA

IV. VLC TRANSMITTER AND RECEIVER

This section details the design of circuits used for data transmission and reception in the VLC link, considering the characterization of the LED luminaire and the photodiode presented in the previous section. The main objective was to design circuits using affordable electronic components readily available in the market. The circuit approach aimed to simplify the design and minimize complexity. These circuits enable the evaluation of the communication capabilities of the VLC system.

A. Transmitter - Tx

The transmitter front-end fulfills two functions: first, it converts the electrical input data signal into an optical output signal, and second, it ensures that LED luminaire operates under the recommended light conditions. Therefore, the transmitter functions as a current controller, allowing the electrical polarization and the modulation of the LED source. The transmitter operates within a current range of 0-300 mA and consists of a Luxeon SP-02-T1SinkPAD-II module with seven LEDs.

A Bias-T circuit is incorporated into the transmitter design, which is a three-port network used to couple an AC signal with a DC signal, as depicted in Fig. 8. The bias-T configuration includes the capacitor C1 to allow the data signal to pass while blocking the DC voltage at low frequencies (60 Hz). The inductor L1 blocks the data signal and allows the DC voltage to pass. Decoupling capacitor C2 ensures stability by eliminating the noise from the voltage source. Finally, the output provides the coupled DC signal and voltage. This arrangement enables the LED luminaire to modulate light while providing indoor illumination. Using a vector network analyzer, the frequency response of the Tx front-end circuit was measured to be approximately 50 MHz at the -3 dB point.

B. Receiver - Rx

The receiver front-end circuit consists of an FDS 100 PIN photodiode, a transimpedance circuit, and a signal gain circuit. Photodiodes (PDs) are devices that convert optical power into electrical current
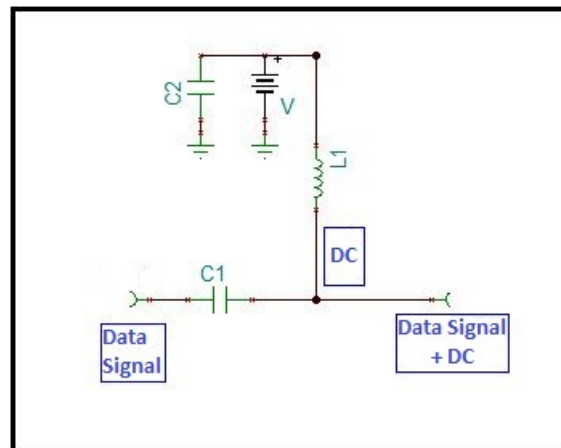
Fig. 8. VLC Transmitter circuit diagram.

and operate in the photoconductive mode with reverse polarization. Therefore, the generated current is directly proportional to the light power incident on the active region of the photodiode (13 mm^2 for the FDS 100 PIN). In this study, the use of a lens was omitted as the focus was on evaluating the performance of the selected photodiode as a communication component. After converting the light into electrical current, it is necessary to convert the current into voltage for signal recovery. A transimpedance amplifier (TIA) is used for this purpose. This amplifier ensures low noise levels in the system and operates over a wide bandwidth [38].

Considering the TIA output, it was determined that additional gain stages were required to amplify the voltage signal, initially in the millivolt range, into volts for subsequent data processing and recovery. The calculations were performed to ensure that the receiving circuit can convert the received photocurrent for values equal to or greater than 2.04 μA. Fig. 9 illustrates the circuit diagram for the receiver front-end, including all the stages. The signal is received by the PD and first amplified by the TIA, providing an output in millivolts. The following three amplifiers constitute the gain stage. Finally, an amplified signal is obtained at the Rx output. The Texas Instruments LMH6629 operational amplifier is used in all stages due to its high speed, ultralow noise, 4 GHz bandwidth-gain product (GBW), and 900 MHz bandwidth. Using a vector network analyzer, the frequency response of the Rx front-end circuit was measured to be approximately 50 MHz at the -3 dB point.
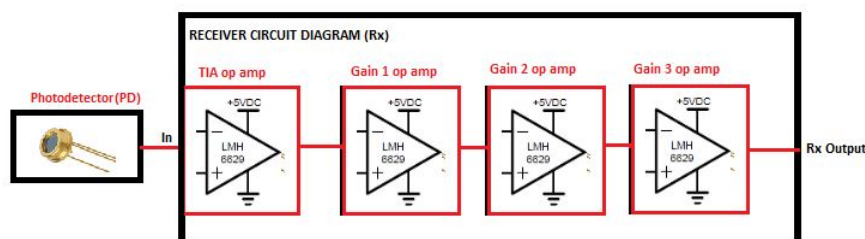

Fig. 9. VLC Receiver circuit diagram.

V. Data Transmission

This section describes data transmission using the designed VLC transmitter and receiver. To validate and verify the operability of the VLC link using the designed circuits, the OFDM and VPPM modulation

techniques were implemented. The performance of the data communication was analyzed at a BER level of $\leq 10^{-3}$. For performances worse than this value the communication is considered inadequate without using error correction codes.

A. Scenario

Table III lists the parameters used for the data transmission. Fig. 10 shows a diagram of the experimental setup and employed equipment.
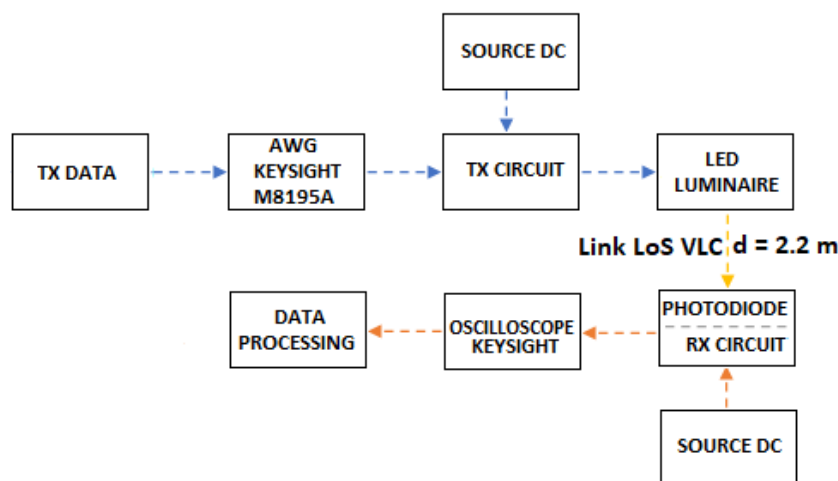

Fig. 10. Experimental setup for testing the data transmission.

In scenario 1, the transmitter and receiver are aligned in an indoor LoS path, the minimum Tx-Rx distance is 0.20 m, and the maximum distance is 2.2 m. Measurements were taken every 0.20 m. At each position, the VLC communication is accomplished, and data are transmitted from the Tx and received at the Rx. At each position, 20 measurements were taken for each of the implemented modulation schemes, then the calculated error was averaged, and the BER versus distance figure of merit was obtained. In scenario 2, the transmitter remained at the same position as in scenario 1, but the receiver was moved laterally from the central position, and the Tx-Rx distance was kept at 2m. This scenario represents a diffuse LoS. The maximum Rx lateral displacement is 1 m with measurements taken every 0.20 m from the central axis. At each point, VLC communication is accomplished, and the BER versus distance is calculated following the same procedure as in scenario 1.

Data are generated by a PC using the MATLAB software and loaded into an arbitrary wave generator (AWG), Keysight model M8195A, which is connected to the transmission circuit. The DC source provided the electrical polarization of the LED luminaire. The receiver circuit was moved along the path according to the chosen scenario. The signal was read by an oscilloscope (Keysight Infiniium, model DSO90404a), and the data were processed offline by a PC. A DC source provided power to the receiver circuit.

B. Data Generation

Transmission was accomplished using VPPM and OFDM modulations. The VPPM data are mapped into a 2-PPM, with two symbols representing bits 0 and 1. Each symbol (pulse) is placed in a time interval, which is obtained by dividing the time allocated to the transmission of a symbol (bit time)

TABLE III. Data transmission link parameters for the VLC system

Parameters	Value	Unit	Scenario 1	Scenario 2
Room size	3x2	m	✓	✓
Optical table size	2x1x1	m	✓	✓
Transmitter Axis		m	0x0	0x0
Receiver Axis		m	2.2x0	2.2x1
Field of view (FOV)	100	degrees	✓	✓
Transmitter half-angle at half power	27	degrees	✓	✓
Distance between LED and PD (min)	0.20	m	✓	✓
Distance between LED and PD (max)	2.2	m	✓	✓
Maximum LED electrical power	[1-6]	W	✓	✓
Scenario	Indoor	–	✓	✓
Path		–	LoS	Diffuse LoS

by M equal intervals. In each interval, one symbol is transmitted. The duty cycle (rc) for each pulse is then configured. For OFDM data transmission, the scheme is shown in Fig. 11. From left to right, the OFDM signal processing is as follows:

- The input data block represents the input bits composed of (0,1);
- The pilot bit block inserts bits whose position is known by the receiving system making it possible to estimate the channel for the equalization process;
- The modulator block is responsible for mapping the bits (0,1) into the 4-QAM constellation;
- The Hermitian block is used to convert complex values into real values, as the LED current needs real values. The QAM modulator delivers symbols of type (± a± jb). These values are obtained from the output of the IFFT block. In this block, the number of carriers was doubled;
- The IFFT block converts the signal from the frequency domain into the time domain, generating a real signal that varies between positive and negative values;
- The cyclic prefix addition block generates a guard interval by copying a portion of the end of the signal and placing it at the beginning of the signal, in order to minimize the inter-symbolic interference (ISI). The P/S block converts parallel data from the serial input into the serial output;
- The signal is generated in the AWG and is transmitted by the LED luminaire to the Rx circuit.

At the receiver, the OFDM signal processing is performed as follows:

- The S/P block is responsible for converting the data from serial format to a parallel sequence;
- The cyclic prefix received at the beginning of the symbol is removed;
- The FFT block transforms the values of the subcarriers that are in the time domain to the frequency domain;
- The equalizer block makes an estimation of the channel so that the received signal can be recovered. The linear least squares (LLS) method was used to obtain the channel response. The received pilot subcarrier was divided by the transmitted subcarrier;
- The demodulator block performs the signal demodulation and oversees the remapping of received symbols into bit values (0,1).
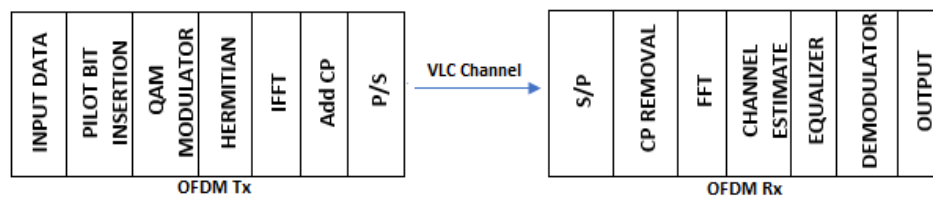
Fig. 11. OFDM Scheme.

Table IV lists the configuration parameters of the OFDM signal.

TABLE IV. Parameters of the OFDM Signal

Parameters	Values
Carriers	512
Data Carriers	192 (37.5 %)
After Hermetian Symmetry	384 (75 %)
Cyclic prefix	128 (25 %)
Number of pilot carriers	64 (12.5 %)
Modulation	4-QAM
Interactions	20

C. Experimental Transmission

The analysis of the data transmission performance in the indoor LoS scenario (laboratory) is presented here. The system was assembled following the scheme shown in Fig. 3 (a) and Fig. 10. By using the designed Tx-Rx circuits, the transmission conditions of the VLC link were evaluated with data recovered at an error rate of BER $\leq 10^{-3}$, while maintaining the lighting conditions detailed in the previous section. For data transmission, the codes generated with the MATLAB software were VPPM (rc= [30, 50, 70, 90] %), which is single-carrier and 4-QAM OFDM, which is a multiple-carrier modulation technique, respectively.

The code was loaded into the AWG (Keysight M8195A) and transmitted over the Tx-Rx link. The evaluation was performed at distances up to 2.2 m. In scenario 1, the Tx-Rx link was horizontally aligned according to the data in Table III. In scenario 2, the Rx circuit was moved laterally, keeping the Tx system fixed according to the data in Table III. The data received by the Rx circuit were analyzed offline. Measurements were performed to determine the highest bit rate for each implemented modulation and its variants. Table V presents the results showing the maximum rate obtained for a signal at a BER $\leq 10^{-3}$ and with a minimum distance of 1.6 m between Tx-Rx, which represents the maximum distance at which the typical illuminance level was achieved (see Table II).

Fig. 12 shows the results of the data rate over distance. The measurements were analyzed considering BER $\leq 10^{-3}$ in scenario 1. For VPPM modulation using rc = 50%, the rate was 12.5 Mbps at d = 1.9m. In the case of rc = 30% and 70%, the achieved rate was 10.5 Mbps in both cases. For 4-QAM OFDM modulation, the rate was 30 Mbps up to a distance of 1.75 m, confirming that the VLC link achieves higher rates for modulation with multiple carriers. Fig. 13 and 14 display the BER performance versus distance with the implemented modulations in scenario 1, aiming to maintain the highest achieved bit rate depicted in Fig. 12.

TABLE V. Experimental measurements - Data rate [Mbps]

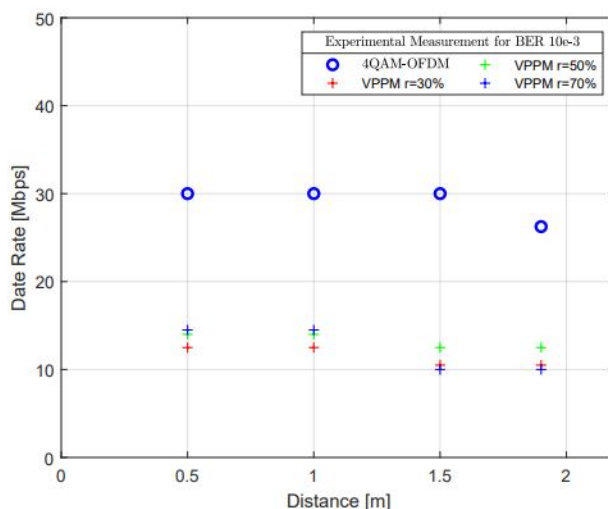| Modulation		Data Rate
VPPM	rc = 30%	10,5
	rc = 50%	12,5
	rc = 70%	10,5
OFDM	with equalization	30

Fig. 12. Data rate for each modulation implemented.

Fig. 13 shows the performance of the communication system based on VPPM modulation configured with different duty cycles (30%, 50%, 70%, and 90%) and with the data rate shown in Table V. The duty cycle determines the time fraction at which the pulse is in an active state. The Fig. 13 shows the measured BER versus distance in scenario 1. For this measurement, different electrical powers were applied to the LED luminaire of the Tx circuit. Results show that the distance at which adequate lighting is guaranteed (approx. 500 lux) in an indoor scenario is 1.6m; therefore, the VPPM modulation with a duty cycle of 30%, 50% and 70% guarantees the communication of the designed VLC system, as shown by the results in Table VI, considering the respective electrical powers applied to the LED.

Fig. 14 shows the performance of the communication link using the 4-QAM OFDM technique configured with 512 subcarriers, which represents a constellation of four symbols. The graph shows the measured BER versus distance in scenario 1 configured with the data rate shown in Table V. It can be seen that for an electrical power of P = 6 W, the BER of $\leq 10^{-3}$ is obtained at 1.75 m using 4-QAM OFDM modulation with LLS and it is achieved at 1.5 m using 4-QAM OFDM modulation without equalization. For the case where the electrical power was P = 3 W, the BER of $\leq 10^{-3}$ is achieved at 1.7 m for 4-QAM OFDM modulation with LLS and at 1.45 m using 4-QAM OFDM modulation without equalization. In this way, and according to measurements made with the luminaire at a distance of 1.6m (approx. 500 lx), adequate communication is guaranteed with the OFDM modulation implemented using 4-QAM modulation with LLS. Fig. 12–14 shows that as the Tx-Rx distance increases, the BER also increases; therefore, to maintain a BER below $\leq 10^{-3}$, the data rate must be decreased.
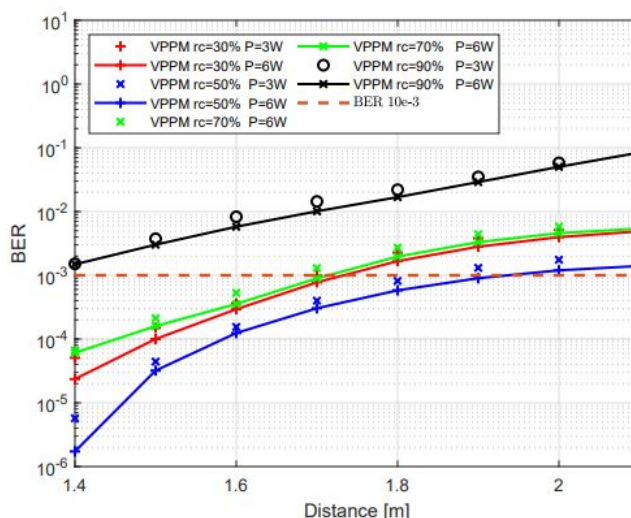
Fig. 13. BER versus Distance plotted for VPPM modulation using different cyclic ratios and electrical power values as configured with the data rate shown in Table V.

TABLE VI. Relationship between distance and maximum achievable data rate for a BER $\leq 10^{-3}$, analyzed with different cyclic ratios of VPPM modulation.

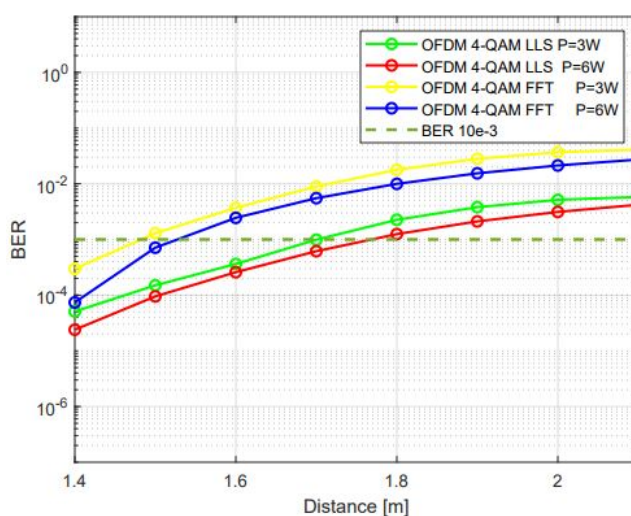| Electric Power	Duty Cycle (%)	Distance (m) with BER$\leq 10^{-3}$
6 W	30	1.75
	50	1.9
	70	1.7
	90	≤ 1.4
3 W	30	1.7
	50	1.8
	70	1.65
	90	≤ 1.4

Fig. 14. BER versus Distance plotted for OFDM modulation using different electrical power values as configured with the data rate provided in Table V.

The SNR of the VLC channel is also estimated using equation (6) based on the data in Table III and the scenarios shown in Fig. 3 (a) and Fig. 3 (b). Fig. 15 illustrates the estimated SNR for scenario 1, considering different electrical powers. The noise was estimated using the parameters of the LED luminaire, photodiode, and electronic circuits. The results show that the highest SNR was obtained for P = 6 W, falling down to ∼8 dB at a distance of 2.2 m. In the case of P = 4 W, an SNR of ∼4 dB was obtained; for P = 2.5 W the value was ∼1.5 dB; and for the case of P = 1 W, the SNR was -20 dB at the same distance of 2.2 m.
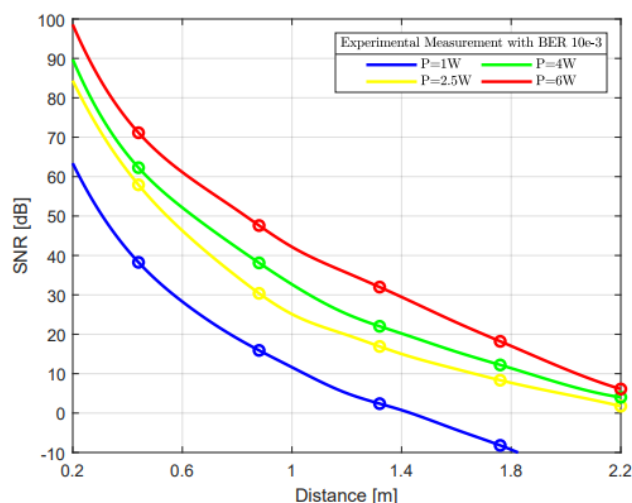

Fig. 15. SNR estimation considering measurements in scenario 1.

Fig. 16 shows the BER behavior in relation to SNR for each implemented modulation and configured for the data rates shown in Table VI, considering measurements in scenario 1. In the case of VPPM modulation, the best performance is achieved with VPPM rc = 50% and with OFDM when the LLS method is implemented.
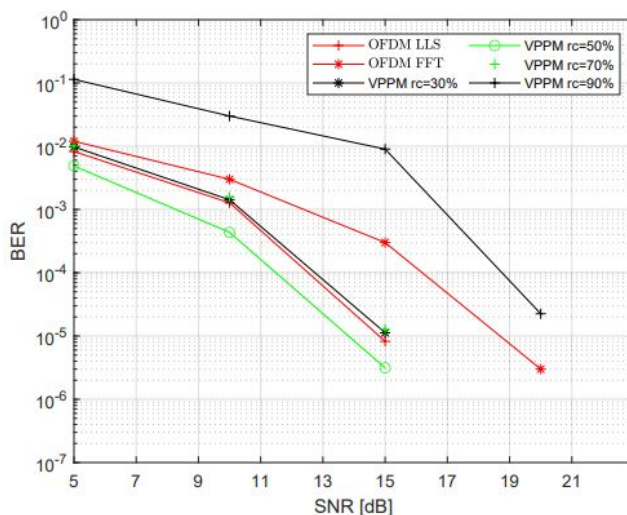

Fig. 16. SNR x BER of scenario 01 with OFDM and VPPM modulations for an electrical power of 6W.

Fig. 17 shows the BER behavior in relation to SNR in scenario 2 (the RX circuit is moved laterally) and for the parameter configuration given in Table III and VI. It is observed that the lateral displacement

worsens the performance of the link compared to the results in Fig. 16. This is related to the attenuation suffered by the signal when there is a displacement that misaligns the Tx-Rx link in the LoS path.
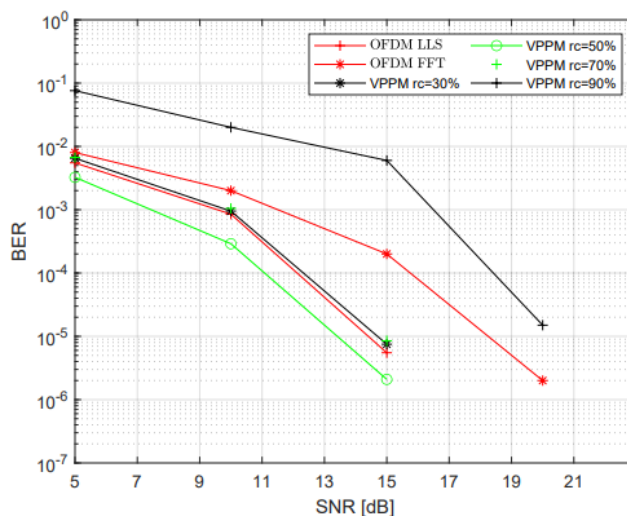

Fig. 17. SNR x BER of scenario 02 with OFDM and VPPM modulations for an electrical power of 6W.

VI. CONCLUSIONS

The approach presented in this work focused on the design of a VLC system, including the characterization of optical components such as the LED luminaire and the photodiode, as well as the design of circuits made with low-cost components readily available in the market. Experimental measurements were conducted, demonstrating the feasibility of achieving a reasonable data rate. We note that comparison with other research works would not be appropriate, as those studies employ non-commercial LEDs, more sophisticated circuits with a higher bandwidth, and solely focus on the VLC communication. Our work focused on the dual VLC functionality using a commercial luminaire. The data rate was limited by the bandwidth of the electronic circuits and the LED luminaire. To achieve a higher data rate, we would need electronic circuits with a greater bandwidth or LED elements with larger bandwidths. However, we must consider that the cost of the system would considerably increase. Therefore, our primary objective was to develop a practical and accessible VLC solution, and we believe that our results effectively support the feasibility of our approach.

Each part of the components and system has been documented. The characterization of the commercial LED luminaire was carried out to find the best performance point that meets the requirements of good lighting according to the illumination standard. The photodiode was also characterized and its operating point was determined. Finally, the data communication link using VPPM and the OFDM modulations was evaluated in order to determine the transmission rates and the performance of the link through BER measurements.

The results show that the designed Tx-Rx circuits, using the commercial LED lamp, fulfill the dual functionality of the VLC system for transmitting information and providing adequate lighting using a commercial LED luminaire driven at different electrical powers. The designed Tx and RX circuits present a bandwidth of 50 MHz at -3 dB. The characterization of the luminaire showed that a single luminaire approximately achieves the performance recommendation for illumination (approx. 500 lux)

in a small office, where the distance between the lamp and the work surface is 1.6 m. Such results are important because they evaluate a real scenario limited by the constrains of the LED luminaire and the receiving circuit. This suggests that to adequately illuminate an entire environment, several luminaires are needed in the room to attend the recommended lighting standards.

On the other hand, for the results with the data link, BER results at $\leq 10^{-3}$ show that in the case of VPPM, the best performance was obtained with a duty cycle of 50%, reaching BER $\leq 10^{-3}$ at 1.9m with a rate of 12.5 Mbps. For the other VPPM configurations the performance worsens, but it still meets the BER of $\leq 10^{-3}$ at 1.6m. For the 4-QAM OFDM modulation, the best performance was obtained at a distance of 1.75 m, reaching a rate of 30 Mbps. We highlight that the implementation of this modulation and the use of equalization significantly improve the performance of the VLC link.

In conclusion, VLC links for indoor can be implemented using LED luminaires previously installed in offices. This work showed that adequate lighting can be maintained and data rates in the range from 12.5 to 30 Mbps can be guaranteed. Higher data rates can be obtained by using LEDs with higher bandwidths and enhanced transmission techniques, such as MIMO.

ACKNOWLEDGMENTS

REFERENCES

[1] X. Li, N. Bamiedakis, X. Guo, J. J. D. McKendry, E. Xie, R. Ferreira, E. Gu, M. D. Dawson, R. V. Penty, and I. H. White, "Wireless visible light communications employing feed-forward pre-equalization and pam-4 modulation," *Journal of Lightwave Technology*, vol. 34, no. 8, pp. 2049–2055, 2016.

[2] A. Al-Kinani, C.-X. Wang, L. Zhou, and W. Zhang, "Optical wireless communication channel measurements and models," *IEEE Communications Surveys & Tutorials*, vol. 20, no. 3, pp. 1939–1962, 2018.

[3] Z. Ghassemlooy, L. Alves, S. Zvánovec, and M.-A. Khalighi, Eds., *Visible Light Communications*. Boca Raton: CRC Press, jun 2017.

[4] D. Karunatilaka, F. Zafar, V. Kalavally, and R. Parthiban, "LED Based Indoor Visible Light Communications: State of the Art," *IEEE Communications Surveys & Tutorials*, vol. 17, no. 3, pp. 1649–1678, 2015.

[5] S. Rajagopal, R. D. Roberts, and S. K. Lim, "IEEE 802.15.7 visible light communication: Modulation schemes and dimming support," *IEEE Communications Magazine*, vol. 50, no. 3, pp. 72–82, 2012.

[6] L. Shi, W. Li, X. Zhang, Y. Zhang, G. Chen, and A. Vladimirescu, "Experimental 5g new radio integration with vlc," in *2018 25th IEEE International Conference on Electronics, Circuits and Systems (ICECS)*, pp. 61–64, 2018.

[7] S. Dimitrov and H. Haas, *Principles of LED Light Communications*, 1st ed. Cambridge: Cambridge University Press, 2015.

[8] H. Burchardt, N. Serafimovski, D. Tsonev, S. Videv, and H. Haas, "Vlc: Beyond point-to-point communication," *IEEE Communications Magazine*, vol. 52, no. 7, pp. 98–105, 2014.

[9] P. A. Haigh, Z. Ghassemlooy, and I. Papakonstantinou, "1.4-mb/s white organic led transmission system using discrete multitone modulation," *IEEE Photonics Technology Letters*, vol. 25, no. 6, pp. 615–618, 2013.

[10] A. H. Azhar, T.-A. Tran, and D. O'Brien, "A gigabit/s indoor wireless transmission using mimo-ofdm visible-light communications," *IEEE Photonics Technology Letters*, vol. 25, no. 2, pp. 171–174, 2013.

[11] R. Bian, I. Tavakkolnia, and H. Haas, "15.73 gb/s visible light communication with off-the-shelf leds," *Journal of Lightwave Technology*, vol. 37, no. 10, pp. 2418–2424, 2019.

[12] Z. Wei, L. Zhang, L. Wang, C.-J. Chen, A. Pepe, X. Liu, K.-C. Chen, Y. Dong, M.-C. Wu, L. Wang, Y. Luo, and H. Y. Fu, "High-speed visible light communication system based on a packaged single layer quantum dot blue micro-led with 4-gbps qam-ofdm," in *2020 Optical Fiber Communications Conference and Exhibition (OFC)*, pp. 1–3, 2020.

[13] D. E. Farfán–Guillén, P. De Tarso Neves Junior, and A. De Almeida Prado Pohl, "Performance evaluation of a los visible light communication link using an optical concentrator and a plano-convex lens," in *2021 Third South American Colloquium on Visible Light Communications (SACVLC)*, pp. 01–06, 2021.

Brazilian Microwave and Optoelectronics Society-SBMO   received 27 Jan. 2023; for review 09 Feb. 2023; accepted 06 Jul. 2023

Brazilian Society of Electromagnetism-SBMag   © 2023 SBMO/SBMag   ISSN 2179-1074

[14] H. Kaushal and G. Kaddoum, "Underwater optical wireless communication," *IEEE Access*, vol. 4, pp. 1518–1547, 2016.

[15] J. Wang, A. Al-Kinani, W. Zhang, C.-X. Wang, and L. Zhou, "A general channel model for visible light communications in underground mines," *China Communications*, vol. 15, no. 9, pp. 95–105, 2018.

[16] T. Yamazato, I. Takai, H. Okada, T. Fujii, T. Yendo, S. Arai, M. Andoh, T. Harada, K. Yasutomi, K. Kagawa, and S. Kawahito, "Image-sensor-based visible light communication for automotive applications," *IEEE Communications Magazine*, vol. 52, no. 7, pp. 88–97, 2014.

[17] M. Uysal, Z. Ghassemlooy, A. Bekkali, A. Kadri, and H. Menouar, "Visible light communication for vehicular networking: Performance study of a v2v system using a measured headlamp beam pattern model," *IEEE Vehicular Technology Magazine*, vol. 10, no. 4, pp. 45–53, 2015.

[18] Y. Zhuang, L. Hua, L. Qi, J. Yang, P. Cao, Y. Cao, Y. Wu, J. Thompson, and H. Haas, "A survey of positioning systems using visible led lights," *IEEE Communications Surveys & Tutorials*, vol. 20, no. 3, pp. 1963–1988, 2018.

[19] L. Feng, R. Q. Hu, J. Wang, P. Xu, and Y. Qian, "Applying vlc in 5g networks: Architectures and key technologies," *IEEE Network*, vol. 30, no. 6, pp. 77–83, 2016.

[20] H. Haas, L. Yin, C. Chen, S. Videv, D. Parol, E. Poves, H. Alshaer, and M. S. Islim, "Introduction to indoor networking concepts and challenges in lifi," *Journal of Optical Communications and Networking*, vol. 12, no. 2, pp. A190–A203, 2020.

[21] D. E. Farfán Guillén, F. César Baraviera Tosta, P. de Tarso Neves, and A. de Almeida Prado Pohl, "Analysis of a vlc link under lighting conditions in an indoor scenario," in *2021 Conference on Lasers and Electro-Optics (CLEO)*, pp. 1–2, 2021.

[22] M. de Oliveira, F. C. B. Tosta, D. E. F. Guillen, P. P. Monteiro, and A. d. A. P. Pohl, "Theoretical and experimental analysis of led lamp for visible light communications," *Wireless Personal Communications*, vol. 125, no. 4, pp. 3461–3477, Aug 2022.

[23] A. Jovicic, J. Li, and T. Richardson, "Visible light communication: Opportunities, challenges and the path to market," *IEEE Communications Magazine*, vol. 51, no. 12, pp. 26–32, 2013.

[24] Luxeon Star LEDs, "SinkPAD-II 7 Rebel LED 40mm Round Module," 2015.

[25] Thorlabs, "Si photodiode fds 100," 0637-S01, Rev M, p. 4, 09 2017.

[26] J. Kahn and J. Barry, "Wireless infrared communications," *Proceedings of the IEEE*, vol. 85, no. 2, pp. 265–298, 1997.

[27] Z. Ghassemlooy, W. Popoola, and S. Rajbhandari, *Optical Wireless Communications: System and Channel Modelling with MATLAB®*. USA: CRC Press, 2012.

[28] S. Idrus, R. Ramirez-Iniguez, and Z. Sun, *Optical Wireless Communications: Ir For Wireless Connectivity*. USA: CRC Press, 01 2007.

[29] T. Komine and M. Nakagawa, "Fundamental analysis for visible-light communication system using led lights," *IEEE Transactions on Consumer Electronics*, vol. 50, no. 1, pp. 100–107, 2004.

[30] Z. Wang, T. Mao, and Q. Wang, "Optical ofdm for visible light communications," in *2017 13th International Wireless Communications and Mobile Computing Conference (IWCMC)*, pp. 1190–1194, 2017.

[31] IEEE, "Ieee standard for local and metropolitan area networks–part 15.7: Short-range optical wireless communications," *IEEE Std 802.15.7-2011*, pp. 1–407, 2011.

[32] I. Standar, "Ieee standard for local and metropolitan area networks–part 15.7: Short-range optical wireless communications," *IEEE Std 802.15.7-2018 (Revision of IEEE Std 802.15.7-2011)*, pp. 1–407, 2019.

[33] M. Afgani, H. Haas, H. Elgala, and D. Knipp, "Visible light communication using ofdm," *2nd International Conference on Testbeds and Research Infrastructures for the Development of Networks and Communities, 2006. TRIDENTCOM 2006.*, pp. 6 pp.–134, 2006.

[34] J. van Wyk and L. Linde, "Bit error probability for a m-ary qam ofdm-based system," *AFRICON 2007*, pp. 1–5, 2007.

[35] J.-H. Yoo and S.-Y. Jung, "Modeling and analysis of variable ppm for visible light communications," *EURASIP Journal on Wireless Communications and Networking*, vol. 2013, pp. 1–6, 2013.

[36] N. Z. J. G. Proakis, M. Salehi and X. Li, *Communication Systems Engineering*, ser. Prentice Hall. New Jersey: Illuminating Engineering Society of North America, 1994, vol. 2.

[37] C. . Committee, "En 12464-1:2011. (revision of en 12464-1:2002) light and lighting - lighting of work places - part 1: Indoor work places," *Light and Lighting Technical Committee*, 2011.

[38] S. B. Alexander, I. of Electrical Engineers, and S. of Photo-optical Instrumentation Engineers, *Optical Communication Receiver Design*, ser. IEE telecommunications series. EUA: SPIE Optical Engineering Press, 1997.